Effect of processing temperature on the structural, electronic and electrical properties of solution-processed amorphous Ge–In–Sn–O thin-film transistors

2014 J. Phys. D: Appl. Phys. 47 085103

(http://iopscience.iop.org/0022-3727/47/8/085103)

IOP Publishing Journal of Physics D: Applied Physics
J. Phys. D: Appl. Phys. **47** (2014) 085103 (6pp) doi:10.1088/0022-3727/47/8/085103

Effect of processing temperature on the structural, electronic and electrical properties of solution-processed amorphous Ge–In–Sn–O thin-film transistors

Jun Hyung Lim[1], Jun Hyuk Choi[1], Seung Muk Lee[1], Byung Du Ahn[2], Kwun-Bum Chung[3], Jin-Seong Park[4], Soo Min Hwang[1] and Jinho Joo[1]

[1] School of Advanced Materials Science and Engineering, Sungkyunkwan University, Suwon 440–746, Korea
[2] School of Electrical and Electronic Engineering, Yonsei University, Seoul 120–749, Korea
[3] Department of Physics, Dankook University, Cheonan 330–714, Korea
[4] Division of Material Science and Engineering, Hanyang University, Seoul 133–719, Korea

E-mail: jinho@skku.edu (J Joo) and redbread@skku.edu (S M Hwang)

Received 2 August 2013, revised 14 December 2013
Accepted for publication 3 January 2014
Published 3 February 2014

Abstract

We report a novel $GeInSnO_x$ (GeITO) thin-film transistor (TFT) synthesized by a solution process, utilizing Ge as a charge carrier suppressor and amorphization-promoter, and the dependence of its microstructure, electronic structure and electrical properties on sintering temperature. The amorphous structure was maintained regardless of the sintering temperature. As the sintering temperature increased, the amount of oxygen vacancies increased and GeO_2 bonds transformed into GeO bonds near the film surface above 400 °C. In addition, the In 5sp/Sn 5sp states appeared to act as the dominant electron source in the GeITO channel layers with increasing sintering temperature. These behaviours influenced TFT performances: the saturation mobility was increased from 0.004 to 6.4 $cm^2\ V^{-1}\ s^{-1}$, while the threshold voltage was shifted in the negative direction by increasing the sintering temperature, which demonstrates the high sensitivity of the solution-deposited GeITO to the processing temperature.

Keywords: oxide semiconductor, thin-film transistor, x-ray absorption spectroscopy

S Online supplementary data available from stacks.iop.org/JPhysD/47/085103/mmedia

(Some figures may appear in colour only in the online journal)

1. Introduction

Amorphous oxide semiconductors (AOSs) have been considered as promising alternatives to organic and Si materials used in thin-film transistors (TFTs) due to their excellent electrical properties and optical transparency [1–3]. Since the study by Nomura *et al* [4] on the next-generation TFTs technology exploring new AOSs compatible with existing poly-Si TFTs with high carrier mobility (50–100 $cm^2\ V^{-1}\ s^{-1}$), considerable efforts have been directed towards the development of AOS TFTs, such as In–Ga–O [5, 6], Zn–Sn–O (ZTO) [7, 8], In–Zn–O (IZO) [9–12], In–Ga–Zn–O [4, 13], In–Sn–Zn–O [14, 15] and Hf–In–Zn–O [16, 17]. Such AOS films have been fabricated mostly by vacuum-based techniques such as pulsed laser deposition [4, 13] and radio-frequency sputtering [5, 7, 9, 16] or solution-based methods such as spin-coating [8, 10, 14, 17] and ink-jet printing [15]. In comparison to the vacuum-based processes, solution-based

approaches would offer great advantages of high-throughput, cost-effectiveness, facile chemical composition control, and possibility of direct printing of materials due to the absence of high-cost equipment and complex photolithography [1]. In this regard, many research groups have recently devoted their efforts to the advancement of solution-processed oxide semiconductors [1, 8, 10, 14, 15, 17].

AOSs are generally comprised of heavy metal cations of large atomic size and $(n-1)d^{10}ns^0$ $(n \geqslant 5)$ electronic configuration, providing high charge carrier mobility even in an amorphous structure [1–4]. Among the various metal cations, both In and Sn have the same $[Kr]4d^{10}5s^0$ electronic configuration and the overlap between the adjacent spherical *ns* orbitals in each of them yields high electron mobility, which can afford highly conductive In- and/or Sn-based AOSs such as In–O, IZO, In–Sn–O (ITO) and ZTO [18, 19]. In addition, it is essential to control the amount of the oxygen vacancies acting as a charge carrier in the channel layers for the realization of robust TFT devices. For example, Kim *et al* reported new TFTs with an amorphous Hf-IZO as an oxide semiconductor layer and suggested that the addition of Hf could suppress growth of the crystalline IZO matrix and control carrier concentration [16]. In addition, Cho *et al* reported an amorphous Al-ZTO TFT with saturation mobility (μ_{sat}) of 10.1 $cm^2\ V^{-1}\ s^{-1}$, subthreshold swing (SS) of 0.6 V/decade, and on/off current ratio (I_{on}/I_{off}) of 10^9 [20]. Fortunato *et al* developed Ga-ZTO TFTs with a high electrical performance (μ_{sat} of 24.61 $cm^2\ V^{-1}\ s^{-1}$, SS of 0.38 V/decade, and $I_{on/off}$ of 10^7 [21]. There have been many similar approaches to date incorporating Zr [22], Hf and Ga in IZO and ZTO matrices aiming at suppressing excess charge carriers.

In this study, Ge, a group IV element, is employed as a new charge carrier suppressor and amorphization-promoter in In–Sn–O (In : Sn = 1 : 3) matrix. Ge is expected to retain its strong bonding with oxygen, thereby suppressing the excessive oxygen vacancies since a Ge–O bond (659 kJ mol^{-1}) is far stronger than those of In–O (395 kJ mol^{-1}) and Sn–O (531 kJ mol^{-1}). Herein, we evaluate the applicability of a novel solution-processed Ge–In–Sn–O (GeITO) TFT by investigating the dependence of its structural, electronic and electrical properties on the processing temperature.

2. Experimental details

The GeITO precursor solution (0.5M) was prepared as follows. Ge isopropoxide $[Ge(OCH(CH_3)_2)_4]$, Sn chloride hydrates $[SnCl_2 \cdot H_2O]$, and In nitrate hydrate $[In(NO_3)_3 \cdot xH_2O]$ were mixed together to obtain an atomic ratio of Ge : In : Sn = 1 : 1 : 3 in the resulting films, and then dissolved in a mixture solvent of 2-methoxyethanol and ethanol (1 : 1 vol%). The precursor sol was stirred for 1 h at room temperature before a small amount of HCl was added as a stabilizer. The solution was deposited by spin-coating at 3000 rpm for 30 s onto heavily-doped p-type Si wafers covered with a thermally grown 100 nm thick SiO_2 layer, subsequently dried at 150 °C on a hot plate and sintered at 250–600 °C for 1 h in ambient air. The atomic ratio (composition) of the films showed the highest sensitivity to sintering temperature,

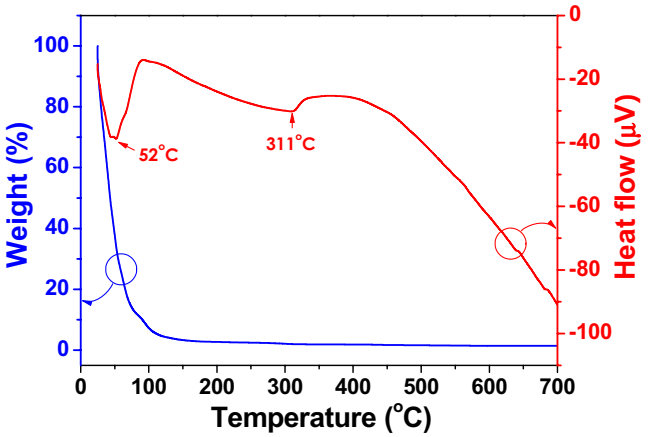

Figure 1. TG/DTA curves of the GeITO precursor solution.

resulting in notable differences in the TFT performances, based on our preliminary experiments, In this study, the actual composition ratio measured by XPS analysis was in the range of 0.93–1.07 : 1 : 2.97–3.25, except for the sample sintered at 250 °C as shown in table S1 of the online supplementary data (stacks.iop.org/JPhysD/47/085103/mmedia). The GeITO films sintered at 250 °C, 300 °C, 400 °C, 500 °C and 600 °C are hereafter denoted as 250-, 300-, 400-, 500- and 600-samples, respectively. Al source/drain electrodes were deposited by thermal evaporation using a shadow mask with a channel width (W) and length (L) of 100 μm and 50 μm, respectively.

The thermal behaviour of the precursor solution was probed by thermogravimetric and differential thermal analyses (TG/DTA, Seiko Exstar 6000) from room temperature to 700 °C at a scan rate of 10 °C min^{-1} in air. The microstructure was observed by high-resolution transmission electron microscopy (HRTEM, JEM2100F, JEOL) and the chemical bonding configuration was checked by x-ray photoelectron spectroscopy (XPS, ESCA2000, VG Microtech) with an Al Kα x-ray source. The electronic structure in the conduction band was investigated by an x-ray absorption (XAS) experiment using the total electron yield (TEY) mode at the soft x-ray beamline, BL-7A Photon Factory, Institute of Material Science, High Energy Accelerator Organization (KEK-PF) in Japan. The electrical properties of the TFT devices were measured by using a semiconductor parameter analyser (HP4145B) at room temperature in air and the μ_{sat} and threshold voltage (V_{th}) were calculated from the drain current-gate voltage ($(I_D)^{0.5} - V_G$) plot.

3. Results and discussion

The TG/DTA curves of the precursor solution are shown in figure 1. The TG curve shows an abrupt weight loss from ~25 to ~150 °C, probably due to the evaporation of the solvent and additives such as 2-methoxyethanol, ethanol and HCl. Then, a gradual weight loss was observed with increasing temperature above ~150 °C. The DTA graph exhibits one sharp endothermic peak at ~52 °C and one broad exothermic region at 311–450 °C. The former peak can be related to the evaporation of the solvent and additive as indicated by the TG

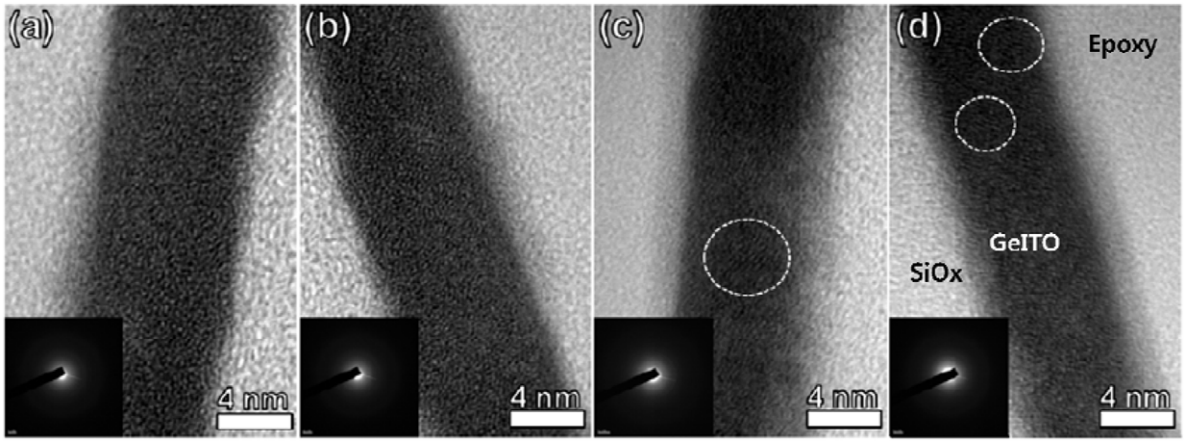

Figure 2. HRTEM images of the GeITO/SiO_2/Si thin films sintered at (*a*) 300 °C, (*b*) 400 °C, (*c*) 500 °C and (*d*) 600 °C. The insets show the corresponding SAED patterns. The dotted circles indicate the local atomic orderings.

data. On the other hand, the latter reaction seems to be due to the formation of the GeITO phase. It is thus speculated that a dense GeITO layer formed at sintering temperatures higher than ~450 °C.

Figure 2 shows the HRTEM micrographs of the GeITO/SiO_2/Si films sintered at 300–600 °C. All the GeITO layers exhibited a film thickness of ~10 nm and amorphous characteristics (see the insets of figure 2 showing halo ring patterns), indicating that the incorporation of Ge in the ITO is effective in sustaining the amorphous structure. However, the local atomic ordering was observed faintly as indicated by the dotted circles in the cases of the 500- and 600-samples (figures 2(*c*) and (*d*)). In general, In–Sn–O (ITO) compounds easily crystallize at lower temperatures [23, 24]. However, in this study, it is thought that the Ge which was incorporated into the ITO matrix inhibited the crystallization of the ITO-based compounds. Thus, the local atomic ordering was probably due to the crystallization of the ITO-rich phases due to local compositional fluctuations.

Figure 3(*a*) depicts the transfer characteristics—a measurement of drain-to-source current (I_{DS}) as a function of gate voltage (V_G) at a fixed drain voltage (V_{DS}) of 20 V by a forward sweep of V_G from −40 V to 40 V—of the GeITO TFTs sintered at different temperatures of 250–600 °C. All the TFTs showed n-channel characteristics and hard drain current saturation at large V_D (see the output curves in figure S1 of the online supplementary data stacks.iop.org/JPhysD/47/085103/mmedia), except the 250-sample whose TFT characteristic was weakly modulated due to the relatively low carrier concentration. The TFT performance parameters, including μ_{sat}, I_{on}/I_{off} and V_{th} and are plotted in figure 3(*b*). It was found that the TFT properties were strongly dependent on the sintering temperature. The 300-sample showed marginal TFT properties such as a μ_{sat} of 0.004 $cm^2\,V^{-1}\,s^{-1}$, I_{on}/I_{off} of 1.2×10^5 and V_{th} of ~13 V. However, increasing the sintering temperature dramatically improved the transfer characteristics. In the 400-sample, a μ_{sat} of 1.2 $cm^2\,V^{-1}\,s^{-1}$, I_{on}/I_{off} of 4.2×10^7 and V_{th} of ~2 V were obtained. When the sintering temperature increased to 500 °C and 600 °C, the μ_{sat} increased to 5.2 $cm^2\,V^{-1}\,s^{-1}$ and

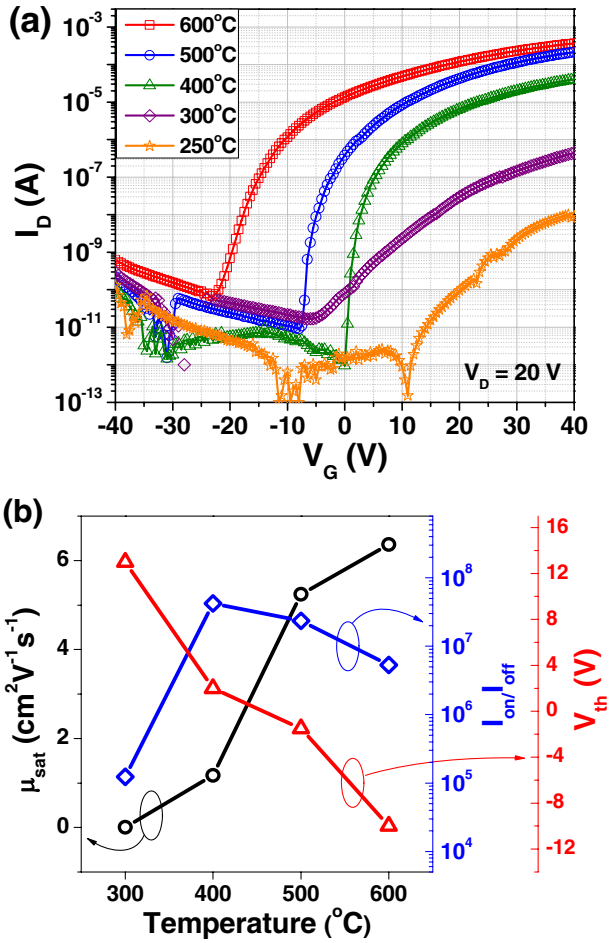

Figure 3. (*a*) Transfer characteristics of the GeITO TFTs sintered at different temperatures and (*b*) variations of the extracted electrical properties such as μ_{sat}, I_{on}/I_{off} ratio, and V_{th} with the sintering temperature.

6.4 $cm^2\,V^{-1}\,s^{-1}$, respectively, whereas the I_{on}/I_{off} degraded slightly and the V_{th} shifted negatively from 13 V to −10 V. Considering that an I_{on}/I_{off} above 10^6 and a SS below 1 are required for high-speed switching TFT devices with low power consumption used in active-matrix liquid crystal

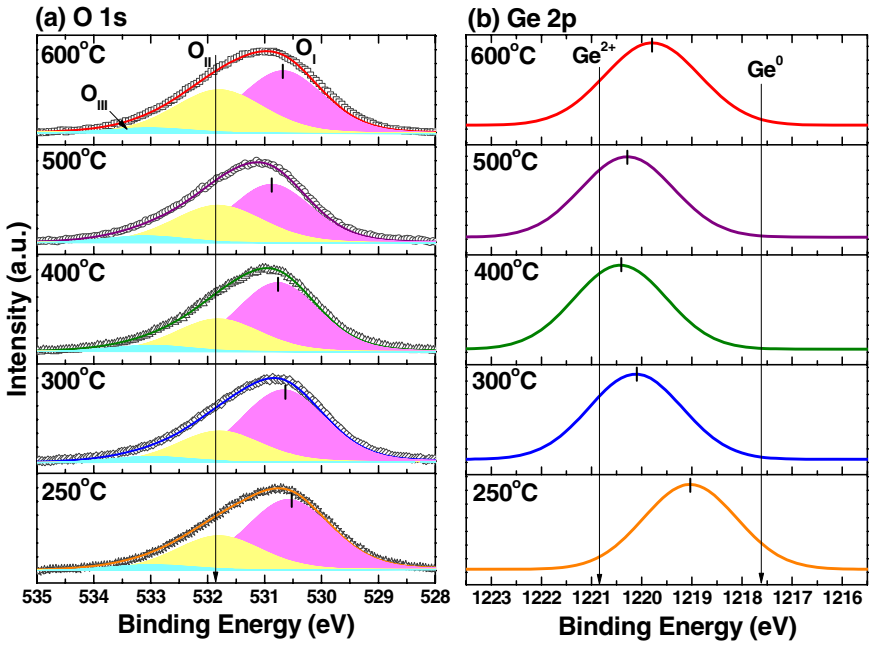

Figure 4. XPS (*a*) O 1s and (*b*) Ge 2p spectra of the GeITO thin films sintered at different temperatures.

displays (AMLCDs) and active-matrix organic light-emitting diodes (AMOLED) displays [1], the 500-sample (with a SS of 0.77 V/decade) was considered as the optimal device in our study, which is in agreement with the aforementioned TG-DTA analysis.

To explore the origin of the variations in the electrical performances with sintering temperature, the electronic structures were analysed by x-ray photoelectron spectroscopy (XPS) and x-ray absorption spectroscopy (XAS). The XPS O 1s spectra of the GeITO films sintered at different temperatures are presented in figure 4(*a*). All the O 1s spectra were deconvoluted into three components using a Gaussian 80%–Lorentzian 20% peak fitting. The low binding energy peak (O_I) at 530.6–530.9 eV and the medium binding energy peak (O_{II}) at ∼531.8 eV are related to the O^{2-} ions in the lattice surrounded by the neighbouring metal cations and to the O^{2-} ions in oxygen-deficient regions, respectively [25–27]. The high binding energy peak (O_{III}) at ∼533.0 eV corresponds to the loosely bonded oxygen on the film surface due to specific chemisorbed species such as $–CO_3$, O_2 or H_2O [25–27]. As the sintering temperature increased from 250 to 500 °C, the binding energy of the O_I component was increased monotonically. This appears to be related to the formation of metal–O bond configurations (oxidation) due to the pyrolysis of the GeITO layer during the sintering. However, the O_I binding energy was decreased slightly after the sintering at 600 °C. In the case of the O_{II} component, whose fraction to total peak area generally reflects concentration of charge carrier (electron) in AOS films, the ratio of relative area to total peak area, $[O_{II}]/[O_{tot}]$, was measured as 0.31, 0.28, 0.31, 0.39 and 0.41 with increasing sintering temperature from 250 °C to 600 °C, respectively. The increase of $[O_{II}]/[O_{tot}]$ indicates that the amount of the oxygen vacancies in the GeITO system was increased when the sintering temperature was increased, resulting in the increase of I_{off} and in the negative shift of V_{th} due to presence of the excess charge carriers in the channel layer [28].

For sol–gel processed metal oxide films, metal hydroxides gradually converts into the metal oxide via thermally-driven condensation processes and the degree of oxide-lattice formation (marked with the O_I) and oxygen deficiency generation (marked with the O_{II}) significantly depend on the sintering temperature [28]. The 250- and 300-samples showed relatively poor TFT properties in comparison to the other samples (figure 3), although no notable differences were found in the XPS O 1s spectra. These results were likely to be due to incomplete dehydration/dehydroxylation processes of the as-coated GeITO layer at the relatively low temperatures, as corroborated by the thermal behaviour of the precursor solution (figure 1). The existence of specific species such as metal hydroxides that resulted from incomplete decomposition can hinder the effective transport of charge carriers [29].

Figure 4(*b*) exhibits the XPS Ge 2p spectra with respect to the sintering temperature. The increase of the sintering temperature up to 400 °C induced a peak shift to the high binding energy, indicating that the electronic structure of the Ge 2p approached GeO_2 (Ge^{2+}; 1220.8 eV) bond configurations [30]. It should be noted that as the sintering temperature increased further to 500 °C and 600 °C, the Ge 2p peak returned to the low binding energy, i.e., the low oxidation state of GeO_x ($0 < x < 2$). On the other hand, for the In $3d_{5/2}$ and Sn $3d_{5/2}$ spectra, both the binding energies were almost constant above 300 °C, regardless of the sintering temperature (not shown). The Ge 2p behaviour was probably due to transformation of GeO_2 to GeO near the film surface at >∼400 °C [30, 31]. The formation of the GeO bond configuration could also affect the electronic structure of the Ge–In–Sn–O system, in particular, the O 1s (O_I and O_{II} components), which was possibly responsible for the regression of the binding energy of the O_I component as well

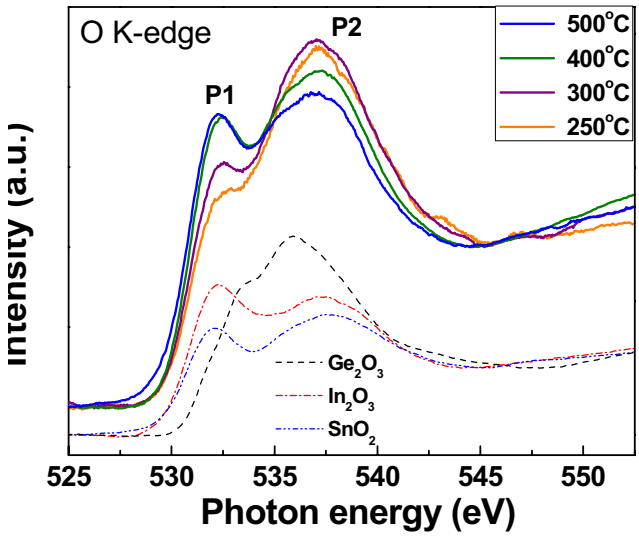

Figure 5. XAS O K-edge spectra of the GeITO thin films for different sintering temperatures.

as the relative increase of the amount of the O_{II} component (oxygen vacancy) with respect to the sintering temperature (figure 4(*a*)).

Figure 5 shows the normalized O K_1 edge spectra of the GeITO films. The spectra of GeO_2, In_2O and SnO_2 binary oxides are also included for comparison. The electronic states of the unoccupied s/p orbitals for GeITO were evaluated approximately, although the peak position, line-shape and intensity of GeITO spectra may be different from those of the binary oxides due to the different local coordination environments. The XAS spectra were carefully normalized by subtracting the x-ray beam background and subsequently scaling pre- and post-edge levels. By this normalization, the qualitative changes of the conduction band could be compared [32]. The O K_1 edge spectra of GeITO were directly associated with the O p-projected states of the conduction band, which consists of unoccupied hybridized orbitals for Ge 4sp, In 5sp, Sn 5sp and O 2p from 530 eV to 550 eV. As can be seen in the figure, the spectra of the conduction band had two distinct peaks. One peak (P1) at ~532 eV was mainly attributed to the In 5sp/Sn 5sp states and the other (P2) at ~536.5 eV was related to the In 5sp/Sn 5sp/Ge 4sp states [33, 34]. The conduction band started to change at 300 °C, and the change became remarkable after 400 °C. As a result, the intensity ratio of P1 to P2 was increased significantly. This behaviour can be explained in relation to the electronic structure of each oxide according to sintering temperature. It has been reported that the GeO_2 species decomposes into GeO on the surface above ~400 °C [30, 31]. The thermal decomposition of GeO_2 can alter the electronic structure of the GeITO system; P2 was diminished. In addition, the electronic structures for In and Sn oxides (In 5sp/Sn 5sp states; P1) was evolved with the increasing sintering temperature, which appears to be the lowest-energy CB state of the GeITO system. Thus, the In 5sp/Sn 5sp electrons would mainly contribute to the conductivity of the GeITO films, leading to the enhancement of the field effect mobility with the increasing sintering temperature, as shown in figure 3. Our results present the effectiveness of the incorporation of Ge as a charge carrier suppressor and amorphization-promoter in the In–Sn–O (In : Sn = 1 : 3) matrix, suggesting a new class (Ge–In–Sn–O) in the channel layers of AOS TFTs for printed electronic devices. For the actual application of the GeITO to devices of AMLCD, reliability issues such as illumination stability under bias stress, leakage current and hysteresis behaviours should be evaluated and improved.

4. Conclusions

We selected Ge as the charge carrier suppressor and amorphization-promoter in a conducting In–Sn–O matrix and studied the microstructure, electronic structure and electrical properties of solution-processed GeITO films according to sintering temperature. The GeITO layers showed amorphous structure and n-channel TFT performances above a sintering temperature of 300 °C. As the sintering temperature increased from 300 to 600 °C, the μ_{sat} increased from 0.004 to 6.4 $cm^2\ V^{-1}\ s^{-1}$ and V_{th} shifted negatively from 13 to −10 V. The high μ_{sat} was probably due to the major contribution of the In 5sp/Sn 5sp electrons to the conductivity of the GeITO films with increasing sintering temperature. In addition, GeO_2 bonds transformed into GeO bonds near the film surface above 400 °C, which tuned the electronic structure of the GeITO system and was partly responsible for the I_{on}/I_{off} degradation, together with the excess oxygen vacancy formation with the increasing sintering temperature. These findings demonstrate that GeITO is a promising channel layer for high-performance TFT devices and the sintering temperature is pivotal in controlling the microstructure, electronic structure and resulting TFT properties. Further studies on optimal film thickness, precursor materials and reliability issues are also required to improve the TFT performances.

Acknowledgments

This research was supported by the Basic Science Research Program through the National Research Foundation of Korea (NRF) funded by the Ministry of Education, Science and Technology (2012-0002923).

References

[1] Fortunato E, Barquinha P and Martins R 2012 *Adv. Mater.* **24** 2945
[2] Jeong J K 2011 *Semicond. Sci. Technol.* **26** 034008
[3] Park J S, Maeng W-J, Kim H-S and Park J-S 2012 *Thin Solid Films* **520** 1679
[4] Nomura K, Ohta H, Takagi A, Kamiya T and Hosono H 2004 *Nature* **432** 488
[5] Presley R E, Hong D, Chiang H Q, Hung C M, Hoffman R L and Wager J F 2006 *Solid-State Electron.* **50** 500
[6] Gonçalves G, Barquinha P, Pereira L, Franco N, Alves E, Martins R and Fortunato E 2010 *Electrochem. Solid-State Lett.* **13** H20
[7] Chiang H Q, Wager J F, Hoffman R L, Jeong J and Keszler D A 2005 *Appl. Phys. Lett.* **86** 013503

[8] Seo S-J, Choi C G, Hwang Y H and Bae B-S 2009 *J. Phys. D: Appl. Phys.* **42** 035106
[9] Dehuff N L, Kettenring E S, Hong D, Chiang H Q, Wager J F, Hoffman R L, Park C-H and Keszler D A 2005 *J. Appl. Phys.* **97** 064505
[10] Koo C Y, Song K, Jun T, Kim D, Jeong Y, Kim S-H, Ha J and Moon J 2010 *J. Electrochem. Soc.* **157** J111
[11] Fortunato E, Barquinha P, Gonçalves G, Pereira L, Martins R and Gonçalves G 2008 *Solid-State Electron.* **52** 443
[12] Yaglioglu B, Yeom H Y, Beresford R and Paine D C 2006 *Appl. Phys. Lett.* **89** 062103
[13] Suresh A, Wellenius P, Dhawan A and Mutha J 2007 *Appl. Phys. Lett.* **90** 123512
[14] Kim M-G, Kim H S, Ha Y-G, He J, Kanatzidis M G, Facchetti A and Marks T J 2010 *J. Am. Chem. Soc.* **132** 10352
[15] Lee D-H, Han S-Y, Herman G S and Chang C-H 2009 *J. Mater. Chem.* **19** 3135
[16] Kim C-J *et al* 2009 *Appl. Phys. Lett.* **95** 252103
[17] Jeong W H, Kim G H, Shin H S, Ahn B D, Kim H J, Ryu M-K, Park K-B, Seon J-B and Lee S Y 2010 *Appl. Phys. Lett.* **96** 093503
[18] Wang L, Yoon M-H, Fracchetti A and Marks T J 2007 *Adv. Mater.* **19** 3252
[19] Miyasako T, Senoo M and Tokumitsu E 2005 *Appl. Phys. Lett.* **86** 162902
[20] Cho D H *et al* 2008 *Appl. Phys. Lett.* **93** 142111
[21] Fortunato E, Pereira L, Barquinha P, Rego A, Gonçalves G, Vilà A, Morante J and Martins R 2008 *Appl. Phys. Lett.* **92** 222103
[22] Park J-S, Kim K, Park Y-G, Mo Y-G, Kim H D and Jeong J K 2009 *Adv. Mater.* **21** 329
[23] Raoufi D, Kiasatpour A, Fallah H R and Rozatian A S H 2007 *Appl. Surf. Sci.* **253** 9085
[24] Gonçalves G, Elangovan E, Barquinha P, Pereira L, Martins R and Fortunato E 2007 *Thin Solid Films* **515** 8562
[25] Fan J C C and Goodenough J B 1997 *J. Appl. Phys.* **48** 3524
[26] Ahn B D, Lim J H, Cho M-H, Park J-S and Chung K-B 2012 *J. Phys. D: Appl. Phys.* **45** 415307
[27] Ishida T, Kobayashi H and Nakato Y 1993 *J. Appl. Phys.* **73** 4344
[28] Jeong S, Ha Y-G, Moon J, Facchetti A and Marks T J 2010 *Adv. Mater.* **22** 1346
[29] Jeong S and Moon J 2012 *J. Mater. Chem.* **22** 1243
[30] Prabhakaran K and Ogino T 1995 *Surf. Sci.* **325** 263
[31] Prabhakaran K, Maeda F, Watanabe Y and Ogino T 2000 *Appl. Phys. Lett.* **76** 2244
[32] Chung K B, Long J P, Seo H, Lucovsky G and Nordlund D 2009 *J. Appl. Phys.* **106** 074102
[33] McGuinness C, Stagarescu C B, Ryan P J, Downes J E, Fu D and Smith K E 2003 *Phys. Rev.* B **68** 165104
[34] Lucovsky G, Zeller D, Wu K and Whitten J L 2011 *Microelectron. Eng.* **88** 1537